Trends in Heat & Mass Transfer
Vol. 13, 2013

Review

Review of homogeneous nucleation boiling phenomena under non-equilibrium heating condition and a generalized model for boiling explosion

Mohammad Nasim Hasan[1] and Masanori Monde[2,*]

[1]Department of Mechanical Engineering, Bangladesh University of Engineering and Technology, Dhaka-1000, Bangladesh. [2]Department of Mechanical Engineering, Saga University, 1 Honjo-Machi, Saga Shi, Saga, 840-0027, Japan

ABSTRACT

In this paper, the homogeneous nucleation boiling phenomena under non-equilibrium liquid heating condition has been reviewed and analyzed by using a recently developed theoretical model. Three different liquid heating cases has been considered in this model, namely (i) linearly increasing boundary temperature condition, (ii) high heat flux pulse heating condition and (iii) constant boundary temperature condition that includes almost all earlier experimental studies of homogeneous boiling under non-equilibrium condition. In this model, a finite liquid control volume or cluster having the size of a characteristic critical embryo at the liquid boundary has been considered and the corresponding energy balance equation is obtained by considering two parallel competing processes taking place inside the liquid cluster, namely, transient external energy deposition and internal energy consumption due to bubble nucleation and growth. Depending on the instantaneous rate of external energy deposition and boiling heat consumption within the liquid cluster, a particular state has been defined as the condition of boiling explosion i.e. the onset of mass scale vaporization in which the bubble generation and its growth causes the liquid sensible energy to decrease. The obtained results have been presented in terms of the average temperature rise within the liquid cluster, maximum attainable liquid temperature prior to the boiling explosion and the time required for achieving the condition of the boiling explosion for various liquid heating cases. With the initial and boundary conditions identical to those reported in literature, model results have been found to be in good agreement with the experimental observations for all of these liquid heating cases. The boiling explosion condition as predicted by the developed model has been verified by comparing the heat flux across the liquid-vapor interface at the boiling explosion with the corresponding limit of maximum possible heat flux, $q_{max,max}$. Also, the limiting condition for the occurrence of homogeneous boiling explosion in water at atmospheric pressure has been determined by applying the present model for any liquid heating condition.

KEYWORDS: homogeneous nucleation boiling, boiling explosion, linear liquid boundary heating, high heat flux pulse heating, liquid contact with high temperature surface, lower limit of homogeneous nucleation boiling

1. INTRODUCTION

In classical thermodynamics, phase transitions are treated as quasi-equilibrium events at a condition corresponding to the saturation state. However, in real phase change phenomena a deviation from

*Corresponding author: monde@me.saga-u.ac.jp

classical thermodynamics occurs under non-equilibrium conditions such as, a liquid super-heating above the boiling point during vaporization. Liquid superheating might be obtained either by heating it rapidly at constant pressure or by depressurizing it rapidly at constant temperature. In either case, the liquid penetrates into a region of non-equilibrium state or metastable state in which the liquid temperature becomes higher than the saturation temperature at the prevailing pressure. The degree of such liquid superheating often ranges from a few tenths of a degree to several tens of degrees, depending on for example; the liquid, the nature of liquid container, the volume of liquid, the purity of liquid and the rate of parametric variation, i.e., liquid heating rate or depressurization rate. In the limiting case of no vapor contact which can be idealized for extremely fast parametric change, it is possible to achieve remarkably high degrees of superheat at which boiling is initiated mainly by homogeneous nucleation of bubbles which is followed immediately by a large scale boiling-usually with explosive force. This instantaneous abrupt phase change phenomenon is technically referred to as boiling explosion or explosive boiling. Boiling explosion resulting from liquid superheating is omnipresent in many industrial as well as natural phenomena. In several industrial processes such as in paper [1], cryogenics [2], and metal processing industries [3], two liquids having different temperatures often come in contact. If the hotter liquid is relatively non-volatile (smelt, molten metal etc.) and the colder liquid is relatively volatile (water, refrigerant etc.), the later can be superheated to a point where it vaporizes rapidly in a massive scale that can cause injury to personnel as well as considerable structural damage [4]. The sudden depressurization of a liquefied gas either intentionally (through the operation of a pressure relief valve) or accidentally (through a loss of containment) can lead to disastrous consequences called BLEVE (Boiling Liquid Expanding Vapor Explosion) accident [5, 6]. Overheating of a reactor's core in nuclear power plant might cause the fuel rod to melt (hot, nonvolatile liquid) and subsequently to interact with the coolant (cold, volatile liquid) thereby leading to the well known molten fuel-coolant interaction [7]. Boiling explosion also occurs when a liquid comes in contact with a hot surface as in the case of jet impingement quenching [8, 9]. While uncontrolled boiling explosion poses a potential hazard, boiling explosion when produced in a controlled manner finds many interesting and practical applications ranging from an ink jet printer [10] to microelectronic cooling devices and micro bubble actuators in MEMS devices [11]. Researches are underway in the technical development of bubble-actuated micro-fluidic devices, such as drug delivery systems [12], vapor bubble micro pumps [13], micro injectors [14], micro thrusters and thermal bubble perturbators [15]. The boiling phenomena associated with these thermal micromachines and MEMS applications differ from usual nucleate boiling in many aspects. First, the bubble nucleation is initiated at a higher temperature close to the theoretical superheat limit. Second, the boiling process is very explosive because the initial bubble pressure is very high. Third, the boiling process is more reproducible because its mechanism is mainly governed by the property of the liquid (i.e., homogeneous nucleation) rather than by the surface characteristics (i.e., heterogeneous nucleation). Successful extraction of the work from high pressure rapidly expanding vapor bubbles generated by microscopic boiling/vapor explosion could revolutionize the design and performance of these above-mentioned thermal micromachines. Therefore, micro scale boiling explosion phenomena has been one of the hot frontier topics in the contemporary heat transfer research and considerable effort has been devoted to a better understanding of the fundamental science and mechanism of boiling explosion phenomena.

1.1. Homogeneous nucleation boiling explosion: From equilibrium viewpoint

The superheat limit of a liquid i.e., the maximum attainable temperature to which a liquid can be heated before it vaporizes spontaneously can be determined theoretically with two different approaches. One approach is based on the mechanical stability consideration of classical thermodynamics and the superheat limit is known as the thermodynamic superheat limit or the spinodal limit, T_{TSL}, which indeed represents the deepest possible penetration of liquid in the

domain of metastable states. At constant pressure and composition, this limit is the locus of the minima in the liquid isotherms, i.e., the spinodal curve of the liquid which satisfies the conditions $(\partial P/\partial V)_T = 0$ and $(\partial^2 P/\partial V^2)_T > 0$. This spinodal curves separates the metastable region which satisfies the mechanical stability condition, $(\partial P/\partial V)_T < 0$, from the unstable region, $(\partial P/\partial V)_T > 0$. In the stable and metastable regions, local density fluctuations damp out with time and therefore the liquid and vapor may remain in its form indefinitely, whereas in the unstable region, even the smallest fluctuation grows up. A typical liquid spinodal curve is illustrated in Figure 1 as the line C–C´–Critical point. The calculated value of the spinodal generally depends upon the equation of state used for the analysis [16]. For instance, using the Van der Waals equation of state, Spiegler *et al*. [17] derived the condition of mechanical stability i.e., the thermodynamic superheat limit, T_{TSL}, as

$$T_{TSL} = 0.844 T_c \tag{1}$$

For fluids at higher pressures up to the critical point, Lienhard [18] proposed the following correlation for the thermodynamic superheat limit, T_{TSL}.

$$\left\{\frac{(T_{TSL} - T_s)}{T_c}\right\} = 0.905 - \left(\frac{T_s}{T_c}\right) + 0.095\left(\frac{T_s}{T_c}\right)^8 \tag{2}$$

where T_c is the critical temperature (K) and T_s is the saturation temperature (K), respectively.

The second approach to describe the maximum liquid superheat temperature is referred to as the kinetic homogeneous nucleation theory [19-21] which bases the temperature and pressure dependence of bubble nucleation on molecular fluctuation probability. At and above saturation condition, molecular fluctuation occurs in such a way to cause a localized decrease in the liquid density, leading to the formation of vapor embryos. The fluctuation probability increases with temperature and at the superheat limit the probability of a high bubble embryo formation rate i.e., a threshold nucleation rate is sufficient to transform the liquid to vapor. This superheat limit is often termed as the homogeneous nucleation temperature or the spontaneous nucleation temperature. According to the classical

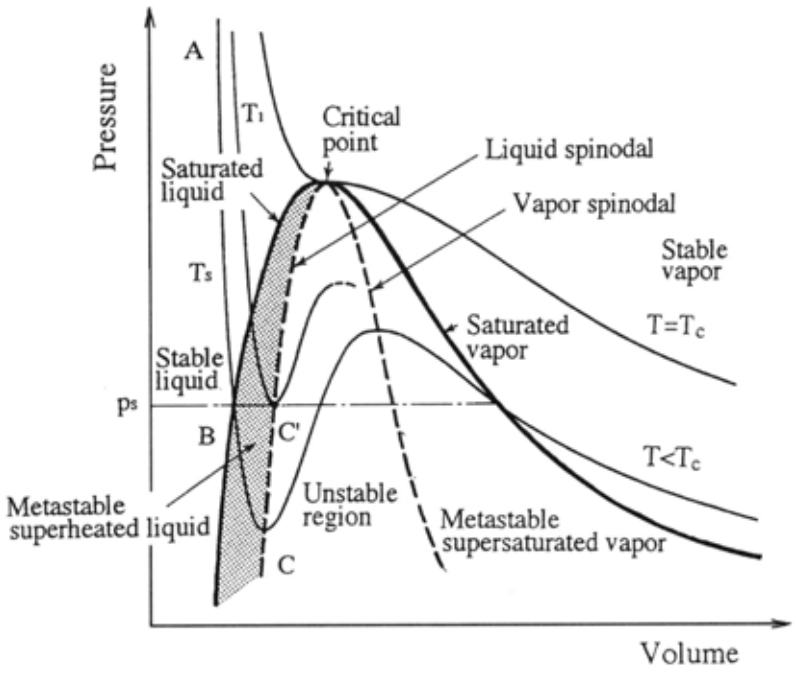

Figure 1. Pressure- volume chart of fluid and the range of metastable superheated liquid.

homogeneous nucleation theory, for a liquid at temperature T_l, the largest nucleation rate, J, per unit liquid volume can be expressed as [21-22]

$$J(T_l) = N_l f \exp\left(-\frac{W_{\min}}{k_B T_l}\right) \quad (3)$$

In Eq. (3), N_l denotes the number density of liquid molecules, f represents the frequency factor and k_B denotes the Boltzmann constant while W_{min} denotes the free energy of formation of a critical nucleus. On further simplification, Carey [23] obtained the homogeneous nucleation rate equation as

$$J(T_l) = N_l \sqrt{\frac{3\sigma}{\pi m}} \exp\left(\frac{-16\pi\sigma^3}{3k_B T_l \{P_s(T_l) - P_0\}^2}\right) \quad (4)$$

where σ, m, P_0 and P_s denote the liquid surface tension, the molecular mass of the liquid, the bulk liquid pressure and the saturation pressure, respectively. Equation (4) can be solved iteratively to determine the kinetic limit of superheat, if a threshold value of J corresponding to the onset of homogeneous nucleation is assumed. From experimental superheat data for a large variety of fluids at atmospheric pressure, Blander and Katz [21] obtained a threshold value of 10^{12} nuclei/(m^3s). As mentioned by Cole [22], a threshold nucleation rate of 10^6 nuclei/(m^3s) gives perfectly acceptable results for the limiting kinetic superheat temperature in most situations. Carey [23] also proposed a value of 10^{12} nuclei/(m^3s) as the threshold nucleation rate.

1.2. Homogeneous nucleation boiling explosion: In experiments

In the laboratory, microscale boiling explosion has been generated and studied usually by heating liquids with thin wires, thin-film microheaters, and high energy laser beams. Fine platinum wire/planar heaters subjected to ramp heating have been extensively used for transient boiling study in earlier research work where the temperature of the wire was determined by the principle of resistance thermometry. Recent advancement in MEMS technology has enabled the fabrication of polysilicon film microheaters with its surface totally free from noticeable cavities in micron or even submicron scale that resulted in the applicability of much high heat flux from the heater surface. Microscale boiling explosion phenomena occurring upon liquid contact with preheated solid surface or during mixing with non-volatile hot liquids has also been addressed by many researchers. A comprehensive review of earlier research work on explosive boiling by using various liquid heating techniques has been done in this paper.

1.2.1. Liquid heating with a linearly increasing boundary temperature

Skripov [24] performed transient boiling experiments on a fine wire under rapid heating in organic liquids and demonstrated that it is possible to superheat the liquid to its homogeneous nucleation temperature, where the molecular energy fluctuations become the dominant mechanism for vapor generation. The condition of explosive boiling named as the impact boiling condition was defined as the minimum heating rate necessary to induce in the liquid the kinetic limit of liquid superheat. Their experiments [25] showed that a heating rate of greater than 6.0×10^6 K/s was required for homogenous nucleation around a platinum heating wire immersed in water at atmospheric pressure. Derewnicki [26] studied transient boiling in water using a thin platinum wire (25 μm diameter) under slow and rapid heating at various system pressures. At a slow heating rate of about 9.0×10^5 K/s and at atmospheric pressure, the bubble nucleation temperature was noted to be about 200°C and only few active heterogeneous nucleation sites were found. On the other hand, at a heating rate of about 6.0×10^6 K/s, the bubble nucleation temperature was obtained to be around 300°C that was found to be relatively independent of the system pressure. Glod *et al*. [27] also investigated the explosive vaporization with a platinum wire immersed in water (10 μm diameter and 1 mm length). At a slow heating rate of 10^5 K/s, the nucleation was found to be initiated by a single vapor bubble growing from a cavity on the wire surface which subsequently triggered the boiling on the entire wire surface with the heterogeneous nucleation being the main mechanism. It was found that the nucleation temperature increased with the heating rate until a maximum limit is reached. At the maximum heating rate of 86.0×10^6 K/s, the wire surface was almost

instantaneously covered with a thin vapor film. A maximum nucleation temperature of 303°C was obtained at the maximum heating rate of 86.0×10^6 K/s when homogeneous nucleation occurred. Iida *et al*. [28-29] experimentally observed the boiling nucleation phenomenon in various liquids (ethyl alcohol, toluene and water) occurring at high boundary heating rates of up to 9.3×10^7 K/s using a small platinum film heater (effective heating area of 100 × 400 μm) that allows simultaneous precise measurement of heater temperature. The heater temperature at the boiling incipience was saturated at approximately 1.0×10^7 K/s for ethyl alcohol and toluene (at approximately 4.5×10^7 K/s for water) and for ethyl alcohol, this value agreed well with the homogeneous nucleation temperature. They found a number of tiny bubbles of uniform size generated immediately after the boiling incipience and the number of generated bubbles tended to increase as predicted by the homogeneous nucleation theory. Okuyama *et al*. [30] investigated the dynamics of boiling process and the spontaneous nucleation on a small film heater immersed in water and ethyl alcohol for much higher boundary heating rates ranging from 10^7 K/s to approximately 10^9 K/s. Under these extreme liquid heating conditions, they found the spontaneous nucleation to be dominant for the inception of boiling. Immediately after the concurrent generation of a large number of fine bubbles, a vapor film was formed by the coalescence that rapidly expanded to a single bubble. With the increase of the heating rate, the coalesced bubble was found to flatten and only a thin vapor film was noticed to grow before cavitation collapse. Avedisian *et al*. [31] measured the average temperature of a Ta/Al heater on a silicon substrate which was immersed in subcooled water during pulse heating at microsecond duration. It was found that the bubble nucleation temperature increased with the heating rate and approached a maximum value of 270°C, corresponding to a maximum heating rate of 2.5×10^8 K/s. Furthermore, the measured nucleation temperature was found in qualitative agreement with the prediction of homogeneous boiling theory for an appropriate value of the contact angle. Kuznetsov and Kozulin [32] experimentally studied the explosive vaporization of a water layer during a temperature rising rate up to about 1.80×10^8 K/s using a microheater (100 × 100 μm) coated with a silicon-carbide layer and recorded the time history of the vaporization process and the dynamics of the steam blanket generated on the heater surface. The observed temperature at the beginning of explosive vaporization over the silicon carbide surface was found to be lower than the spinodal temperature.

1.2.2. Liquid heating with a high boundary heat flux

Asai *et al*. [33-35] conducted a series of theoretical and experimental studies on bubble nucleation and growth in water-based ink and methyl alcohol under the typical operating condition of thermal ink jet printer. A one dimensional numerical model of bubble growth and collapse and the resulting flow motion on a typical bubble jet printing head (effective heating area 150 × 30 μm) was presented by Asai [33]. Later, Asai [34] presented another theoretical model to predict the nucleation process in water-based ink. In his model, nucleation probability was derived and used to simulate the initial bubble growth process. Model prediction was confirmed by experimentations conducted with a prototype bubble jet printing head (effective heating area 150 × 30 μm) for heat fluxes ranging from 100 MW/m^2 to 200 MW/m^2. Asai [35] also described another model of bubble dynamics under high heat flux pulse heating conditions. The proposed model was validated by experimentation using a thin film heater (100 × 100 μm) for methanol heating with high heat fluxes ranging from 5 to 50 MW/m^2. From agreement between experimental result and theoretical prediction, they implied that the dominant bubble generation mechanism was the spontaneous nucleation of liquids due to thermal fluctuation, i.e., the homogeneous nucleation. Yin *et al*. [36] studied the bubble nucleation process in FC-72 on an impulsively powered square microheater (260 × 260 μm) for pulse widths of 1-10 ms duration at different heat fluxes between 3 and 44 MW/m^2. At a low heat flux of 3.43 MW/m^2, a single large bubble consistently appeared near the center of the heater that grew very dynamically overshooting its equilibrium size, shrinked and then essentially stabilized over the heater while at high heat flux of 44 MW/m^2, and nucleation

occurred at several spots on the heater. Varlamov *et al*. [37] experimentally observed explosive boiling of liquids (water, toluene, ethanol, and isopropyl alcohol) on film heaters under the action of pulse heat fluxes of 100-1000 MW/m^2 by using stroboscopic visualization technique with a time resolution of 100 ns. From their observation, they figured out the specific conditions of thermal effect (magnitude of heat flux, duration and repetition frequency of the heat pulse), which ensure single and repeated boiling, intermittent boiling, and boiling with formation of complicated multi-bubble structures. From the experimental data and their comparison with theoretical prediction, they concluded that homogeneous nucleation was the dominant mechanism for boiling in all liquids under consideration for heat fluxes higher than 100 MW/m^2. Hong *et al*. [38] carried out the experimental study of the rapid formation and collapse of bubbles formed on a microheater (25 × 80 μm) induced by pulse heating. In this study, a high heat flux of more than 750 MW/m^2 was applied to the resistive heater with the pulse heating duration being varied from 1 to 4 μs. From experimental observation, they mentioned a threshold pulse duration above which the maximum size of the bubble does not change anymore. They obtained the nucleation temperature for water slightly below the theoretical superheat limit and found a weak linear dependency on the heating rate. They mentioned the mechanism of the bubble formation to be a combined homogeneous- heterogeneous nucleation. Xu and Zhang [39] studied the effect of pulse heating parameters on the micro bubble behavior of a platinum microheater (100 × 20 μm) immersed in a methanol pool with heat fluxes of 10-37 MW/m^2 and pulse frequency of 25-500 Hz. The boiling incipience temperature was found as the superheat limit of methanol corresponding to the homogeneous nucleation.

1.2.3. Liquid heating during contact with hot liquid/solid

The boiling explosion phenomena occuring in a liquid-liquid system is often known as the vapor explosion. Henry and Fauske [40] identified the necessary conditions for the occurrence of the boiling explosion phenomena in liquid-liquid systems as (i) the threshold temperature for spontaneous nucleation in the cold liquid, (ii) the existence of stable film boiling to sustain vapor embryos of the critical size prior to boiling explosion, (iii) the size of cold liquid drops exceeding a critical value to be captured by the hot liquid surface, and (iv) the interfacial temperature between the two liquids exceeding the homogeneous nucleation temperature. Ochiai and Bankoff [41] proposed the 'splash' theory, which states that splash (instantaneous boiling or vapor explosion) occurs within the temperature range, $T_{sn} < T_i < T_c$ where T_{sn} and T_c denote the spontaneous nucleation temperature and the critical temperature of the cold liquid while T_i denotes the interfacial temperature between the two liquids in contact. Iida *et al*. [42] conducted experiments on vapor explosion resulting from mixing of a molten salt drop such as LiCl or $LiNO_3$ in water. They observed that stable film boiling and $T_i > T_{sn}$ were necessary conditions for vapor explosion in the molten salt-liquid system. They also mentioned that both the hot and cold liquids had the upper and lower temperature limits for vapor explosion.

While researches on boiling explosion by using ultra thin heating wire and thin film microheater focused on the mechanism of boiling nucleation and growth, the potential of exploding vapor to perform work on the surrounding bulk liquid etc., research on the boiling phenomena upon liquid contact with a hot surface has been found to pose a significantly different issue, that is when liquid can wet a hot surface. The limiting condition under consideration has been described in varieties of ways such as the minimum film boiling (MFB) temperature, minimum heat flux (MHF) temperature or the temperature of film boiling destabilization etc. Some other scientists also addressed the similar phenomena with other synonyms that include the rewetting temperature, the Leidenfrost temperature etc. However, the Leidenfrost temperature still remains a poorly understood phenomenon in the context of solid-liquid contact heat transfer. Spiegler *et al*. [17] described the rewetting temperature in terms of the maximum superheat temperature of the liquid because above this temperature the liquid would immediately boil explosively and thus could not touch the surface. For instance, Spiegler *et al*. [17] considered the maximum superheat limit as the

spinodal limit obtained by using the Van der Waals equation of state for the liquid as shown in Eq. (1), while the interfacial liquid temperature has been approximated by infinite slab model which considers that both the solid and liquid behave like two semi-infinite slabs of uniform initial temperatures that are suddenly brought into contact. Gunnerson and Cronenberg [43] proposed a thermodynamic model for the prediction of the temperature for film boiling destabilization and discussed its relation with vapor explosion phenomena. In their model, they also considered the solid-liquid contact phenomena as a two 1-D semi-infinite body contact problem. For a perfectly smooth surface, they considered the boiling to occur at an interfacial temperature being equal to the maximum liquid superheat while for imperfect interface, they assumed the boiling to occur at a minimum interfacial temperature being equal to the liquid saturation temperature at the prevailing pressure. Gerweck and Yadigaroglu [44] studied the liquid to vapor transition process that occurs when the liquid comes in to contact with a hot wall. They used statistical mechanics to derive an approximate local equation of state for the fluid as a function of distance from the wall. They arrived at a wall rewetting condition different from the minimum film boiling temperature. They defined the rewetting temperature as the temperature at which the liquid can touch the wall without being immediately turned into vapor. The immediate phase change denoted herein referred to the explosive vaporization of the liquid near the maximum liquid superheat. They concluded that the spinodal temperature is a good estimation for the maximum superheat temperature that a liquid can sustain on a wall for most situations encountered in rewetting experiments. Inada and Yang [45] experimentally observed the boiling phenomena of single water drops upon impingement on a heated surface. Vapor micro-explosions were captured by a high-speed video camera. Measurements were made for the frequency and amplitude of the elastic longitudinal waves produced by boiling and the acoustic pressure of boiling sound. They found the maximum frequency and amplitude of the elastic-longitudinal waves and the maximum values of the boiling acoustic pressure to occur in a certain range of the surface temperatures for violent miniaturization of sessile drops. Moreover, the range of the surface temperatures coincided with that of the transition-boiling regime around the homogeneous nucleation temperature of the liquid. They described the miniaturization phenomena to be induced by an explosive boiling resulting from a direct contact between parts of the liquid and the heating surface. Woodfield *et al*. [8] used a high-speed video camera and microphone to capture the flow behavior and boiling sound of a free-surface water jet impinging on a high temperature surface during quench cooling. Depending on the surface superheat, Woodfiled *et al*. [8] obtained different flow patterns. For the cases where the initial surface temperature was above about 300°C, an almost explosive flow pattern appeared which was in contrast to slightly lower temperatures where a liquid sheet flow structure was apparent. This change in flow phenomena was accompanied by a sudden change in the boiling sound and an increase in the heat transfer rate. Islam *et al*. [9] also mentioned that the occurrence of boiling explosion due to homogeneous and/or heterogeneous nucleation boiling hinders the establishment of the stable solid-liquid contact during jet impingement quenching. Their observation also revealed that a stable solid-liquid contact during jet impingement quenching only occurs when the surface temperature is cooled down below a certain limit when no boiling explosion occurs as indicated by a visible “wet patch” on the hot surface beneath the impinging jet.

1.2.4. Motivation for a new model

Most of the previous studies on explosive boiling following rapid liquid heating have focused on the incipience condition of bubble generation, the mechanism of boiling nucleation, and the effect of rapid oscillation of bubble growth and collapse on liquid motion. The condition of boiling incipience and that of boiling explosion are quite different and which condition corresponds to the boiling explosion remains unclear. A clear understanding of the boiling explosion condition is necessary in order to better predict the frequency of boiling-actuated devices and to improve micro-heater design. It is also important to understand the cooling phenomena at the early stages of jet impingement quenching. For various practical

reasons, ascertaining the boiling explosion condition experimentally for different heating conditions is difficult and sometimes almost impossible especially at extremely high rates of liquid heating. The theoretical model described by Elias and Chambre' [46] seems inadequate to handle the process of transient non-uniform liquid heating as it does not take into account the liquid thickness which is enough for the boiling explosion to take place. So it is important to develop a new model by taking account of an appropriate liquid volume for the treatment of realistic transient non-uniform liquid heating cases. Most recently, a theoretical model [47] has been developed for the process of rapid, non-uniform transient liquid heating and subsequent boiling explosion. Based on the instantaneous energy consumption rate of bubble generation and growth by homogeneous nucleation, a particular state of liquid heating has been defined as the boiling explosion condition in this model [47] which will be briefly explained and summarized in the next chapter.

2. New model for boiling explosion

In this model, a liquid control volume or cluster is considered on the liquid-solid interface as shown in Figure 2 where heat has been stored by conduction, while some of the stored heat in the cluster will be consumed to generate bubbles. The cluster size is much smaller than a macroscopic observed event so that what takes place around the cluster may be treated as one dimensional semi-infinite heat conduction in the stagnant liquid. As the liquid temperature field is transient and non-uniform, the determination of the cluster size becomes very important. For instance, Carey [23] proposed the following equation for the radius of equilibrium critical vapor embryo (r_c) in a superheated liquid (T_l):

$$r_c = \frac{2\sigma(T_l)}{P_s(T_l)\exp\left[\{P_o - P_s(T_l)\}/\rho_l R T_l\right] - P_o} \qquad (5)$$

Equation (5) gives a critical condition for whether the embryo will spontaneously grow or not depending on whether it becomes larger than the size of $r = r_c$ or not with an energetic point of view against meta-stable bubbles. The variation of the radius of critical vapor embryo, r_c, with the liquid temperature, T_l, can be calculated by Eq. (5) and is shown in Figure 3 for water at atmospheric pressure. As depicted in Figure 3, r_c decreases gradually with increasing liquid temperature. In this model, we adopt this embryo size ($2r_c$) at maximum liquid superheat (T^*_{avg}) as the cluster size (x_e) i.e., $x_e = 2r_c$ in the liquid. The net increase in the internal energy of the liquid cluster depends on transient energy deposition as well as transient energy consumption due to bubble nucleation and growth, which can be obtained in terms of the average temperature in the liquid cluster as follows:

$$\frac{dT_{avg}}{dt} = \frac{d}{dt}\left(\frac{1}{x_e}\int_0^{x_e} T(x,t)dx\right) = \frac{1}{\rho_l c_l x_e}\left[q_d(t) - q_c(t)\right] \qquad (6)$$

This model defines whether the homogeneous nucleation boiling explosion takes place or not,

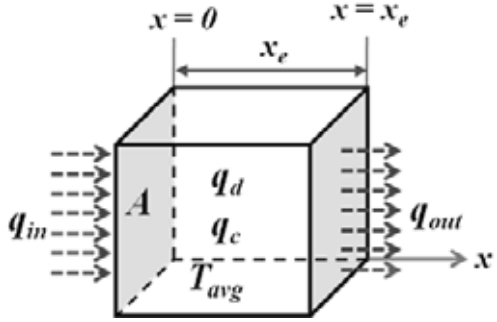

Figure 2. Schematic of the liquid control volume/cluster.

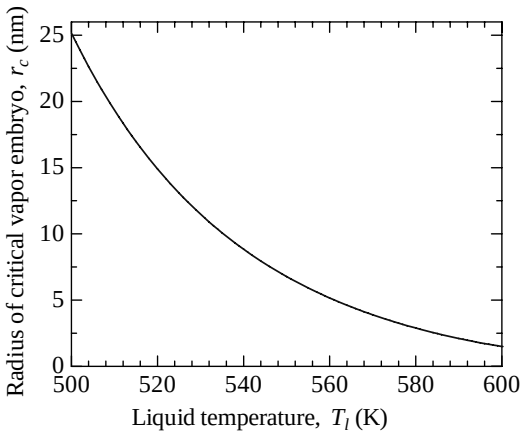

Figure 3. Radius of critical vapor embryo (r_c) at various liquid temperatures for water at atmospheric pressure.

depends on whether $dT_{avg}/dt < 0$ or not. In other words, if, $dT_{avg}/dt > 0$, then the heat still continues to be stored, while, if, $dT_{avg}/dt < 0$, then the necessary heat consumption for the generation and growth of the bubbles, becomes at a moment, larger than the amount of external heat supply. At this moment, the huge amount of heat consumption would bring the liquid superheat into a catastrophic vaporization, namely, a state called boiling or vapor explosion. The corresponding time at the onset of the condition, $dT_{avg}/dt = 0$, with the attainable limit of cluster temperature is denoted by t^*, as the time of homogeneous boiling explosion.

The rate of energy deposition in the cluster, $q_d(t)$, due to heat conduction can be obtained from the difference in heat fluxes across the cluster as

$$q_d(t) = -\lambda_l \left\{ \left.\frac{\partial T}{\partial x}\right|_{x=0} - \left.\frac{\partial T}{\partial x}\right|_{x=x_e} \right\} \tag{7}$$

In order to calculate the heat fluxes on both sides of the liquid cluster as in Eq. (7), we need a boundary condition for the cluster, for which one-dimensional heat conduction can be solved. We may focus three different boundary conditions such as linearly increasing temperature condition [27-30] or constant temperature condition like jet impingement quenching [8, 9] or a constant high heat flux condition [33-35, 37, 38].

The rate of energy consumption, $q_c(t)$, due to vaporization inside the cluster, x_e, can be expressed as

$$q_c(t) = x_e \Gamma_G(t) L \tag{8}$$

where L denotes the latent heat of vaporization and $\Gamma_G(t)$ represents the rate of vapor mass generation per unit mixture volume. It is noteworthy that only the homogeneous nucleation boiling has been considered; i.e., boiling occurs without any cavity or surface effect. With the assumption that all bubbles generated in different stages of liquid heating grow up independently, the vapor generation rate, $\Gamma_G(t)$, can be calculated from the number of generated vapor bubbles and their growth according to the following integration:

$$\Gamma_G(t) = \int_0^t \left\{ 4\pi r^2 \frac{\partial r(t,t')}{\partial t} \rho_v \right\} J(T_l(t'))dt' \tag{9}$$

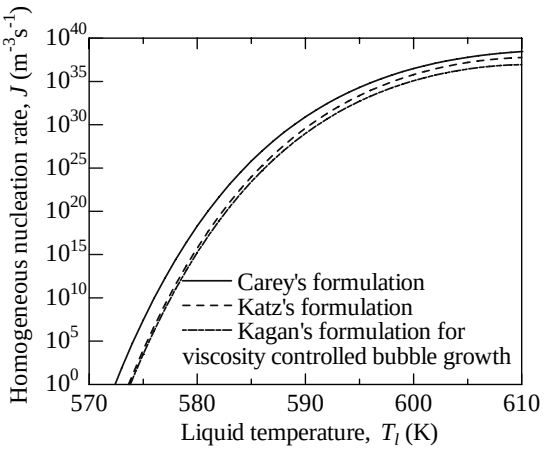

Figure 4. Homogeneous nucleation rate vs. liquid temperature for water at atmospheric pressure.

For the number of bubbles, Carey [23] proposed the rate of homogeneous nucleation events per unit volume in a superheated liquid at temperature, T_l, as

$$J(T_l) = 1.44 \times 10^{40} \sqrt{\frac{\rho_l^{\,2}\sigma}{M^3}} \exp\left(-\frac{1.213 \times 10^{24} \sigma^3}{T_l \{P_s(T_l) - P_0\}^2} \right) \tag{10}$$

Blander and Katz [21] and Kagan [48] also derived similar expressions for J. Figure 4 shows the variation of the nucleation event rate, J, with liquid temperature, T_l, for water at atmospheric pressure. The trend of variation of J with T_l is similar in all cases, i.e., there is a very narrow temperature range below which homogeneous nucleation rate does not occur while above which it occurs instantaneously.

Next, for the bubble growth, Skripov [24] proposed

$$r(t,t') = \phi\sqrt{t - t'} \tag{11.a}$$

$$\phi = 2\sqrt{\frac{3}{\pi}} \frac{\sqrt{\lambda_l \rho_l c_l}}{L\rho_v} (T_l - T_s) \tag{11.b}$$

where, $r(t, t')$ denotes the radius of a bubble at any time, t, which has been created at a time, t'. Upon substituting Eq. (11) in Eq. (9) and substituting T_l for T_{avg}, the expression of the instantaneous vapor generation rate per unit mixture volume, $\Gamma_G(t)$, can be obtained as a function of the average liquid temperature, T_{avg}, as follows:

$$\Gamma_G(t) = 2\pi \int_0^t J(T_{avg}) \phi^3(T_{avg}) \rho_v \sqrt{t-t'}\, dt' \qquad (12)$$

Although J, ϕ and ρ_v in Eq. (12) depend on the average liquid temperature, T_{avg}, the dependence of the nucleation rate, J, on T_{avg} is particularly important due to the existence of σ and P_s in the exponential term. As some terms weakly depend on the liquid temperature, all terms other than the nucleation rate are taken out of the integral for simplicity. Finally, the following equation has been obtained for the instantaneous rate of boiling heat consumption due to homogeneous nucleation boiling, $q_c(t)$:

$$q_c(t) = 2\pi L \phi^3(T_{avg}) \rho_v x_e \int_0^t J(T_{avg}) \sqrt{t-t'}\, dt' \qquad (13)$$

By incorporating the expressions of $q_d(t)$ and $q_c(t)$ in Eq. (6), the following intrego-differential equation can be finally obtained for the average liquid temperature, T_{avg}, over the cluster of a characteristic size, x_e, with the consideration of simultaneous homogeneous nucleation boiling during non-equilibrium liquid heating:

$$\frac{dT_{avg}}{dt} = \frac{1}{\rho_l c_l x_e} \left[\begin{array}{l} -\lambda_l \left\{ \left.\dfrac{\partial T}{\partial x}\right|_{x=0} - \left.\dfrac{\partial T}{\partial x}\right|_{x=x_e} \right\} \\ -2\pi L \phi^3(T_{avg}) \rho_v x_e \displaystyle\int_0^t J(T_{avg}) \sqrt{t-t'}\, dt' \end{array} \right] \qquad (14)$$

The initial condition for Eq. (14) corresponds to $T_{avg} = T_0$ at $t = 0$. The given governing equation, i.e., Eq. (14), together with Eq. (5) (for $x_e = 2r_c$ with T_l replaced by T_{avg}) is complete enough for the closed form solution, if the temperature distribution in the liquid is given.

3. Procedure of calculation

At first, any arbitrary thickness of the liquid control volume for instance, x_{ei} is assumed with the average temperature, $T_{avg} = T_0$ at $t = 0$. For this arbitrarily chosen liquid control volume thickness, x_{ei}, the temporal variation of the average liquid temperature, T_{avg}, is then obtained by calculating the instantaneous energy deposition rate, $q_d(t)$ and energy consumption rate due to boiling, $q_c(t)$ in the liquid control volume as per Eq. (7) and Eq. (8), respectively. Note that the average temperature in the liquid volume may increase ($dT_{avg}/dt > 0$) or decrease ($dT_{avg}/dt < 0$) depending on the relative magnitude of instantaneous energy deposition rate, $q_d(t)$ and energy consumption rate $q_c(t)$ in the liquid cluster. How the average temperature in the liquid cluster will vary with time will be shown later for various liquid heating conditions. With the simultaneous external energy deposition, $q_d(t)$, and internal energy consumption due to boiling, $q_c(t)$, eventually a stage is reached at $t = t^*$, ($dT_{avg}/dt = 0$) at which $q_c(t)$ becomes equal to $q_d(t)$ with the maximum attainable liquid temperature in the cluster, $T_{avg} = T^*_{avg}$. This specific stage of bubble generation and growth has been defined as the boiling explosion in the present model after which further bubble nucleations and their growth immediately cause the liquid sensible energy to decrease ($q_c(t) > q_d(t)$ and $dT_{avg}/dt < 0$). The maximum attainable temperature in the cluster, T^*_{avg}, obtained for x_{ei} is then used to calculate the size of the critical vapor embryo, $2r_c(T^*_{avg})$, as per Eq. (5) which is considered as the liquid control volume thickness or cluster size, x_e, for the next iteration. This iteration procedure is repeated until it converges, that is, the absolute value of $(x_e - x_{ei})/x_{ei}$ becomes less than 0.0001. Finally, the temperature rise in the liquid cluster is obtained for the cluster thickness, x_e, and the boiling explosion characteristics such as the liquid temperature limit (T^*_{avg}), the time (t^*) at the boiling explosion ($q_c(t) = q_d(t)$ and $dT_{avg}/dt = 0$) are determined.

4. Application of the new model to specified conditions

In order to calculate the change of the average temperature given by Eq. (14) from a complete set of Eqs. (5) to (13), one first has to choose a specified boundary condition related to the boiling explosion phenomenon, which has been generally encountered during a rapid rise in liquid temperature by a direct heating of liquid and by a contact of liquid with high temperature solid as mentioned before. Therefore, this model may be applied to three different liquid heating cases namely, (1) liquid heating with linearly increasing temperature, (2) liquid heating at high heat flux pulse heating and (3) a contact of liquid with high temperature solid. Note that the initial and boundary conditions of liquid heating cases under consideration are identical to some of the earlier experimental work reported in literature.

4.1. Solutions for three different conditions

The governing equation for heat conduction in the semi-infinite stagnant liquid becomes

$$\frac{\partial T}{\partial t} = a\frac{\partial^2 T}{\partial x^2} \quad \text{for } 0 < x \tag{15}$$

with a uniform temperature distribution of $T = T_0$ at $t = 0$. Provided that the boundary condition is given, Eq. (15) can be solved. The solutions can be summarized depending on the three different boundary conditions as given in the Table 1 [49]. The solutions for the different boundary conditions are applied to predict the homogeneous nucleation boiling phenomena by combining them with Eqs. (5) to (13).

4.2. Linearly increasing temperature

Four different heating rates for water heating at atmospheric pressure have been considered here with the identical initial and boundary conditions reported by Glod *et al*. [27], Iida *et al*. [29], and Okuyama *et al*. [30]. In these studies, the rate of boundary temperature increase ranges from $b = 37.3\times10^6$ K/s to 1.80×10^9 K/s. As one of the examples, we choose the case of $b = 37.3 \times 10^6$ K/s [29] and then calculate the temporal variation of average liquid temperature, T_{avg}, along with the transient rates of external heat deposition, $q_d(t)$, and boiling heat consumption, $q_c(t)$, within the cluster which are shown in Figure 5. Figure 5(a) indicates that the deposited energy causes only sensible heating of the liquid during most of the heating process. No boiling heat consumption occurs until the liquid temperature reaches a certain value because homogeneous nucleation occurs only when the liquid temperature reaches a certain temperature as shown in Figure 4. Once boiling is initiated, the rate of boiling heat consumption increases sharply as the rate of homogeneous nucleation increases exponentially with liquid temperature. Upon closer observation on Figure 5(b), which depicts the boiling phenomena on a magnified time scale, the rate of homogeneous boiling heat consumption in the cluster increases by over six orders of magnitude within approximately 0.10 μs after the commencement of homogeneous nucleation boiling. Increased boiling heat consumption at higher liquid temperature in turn slows the rate of liquid temperature escalation. As a result of these two mutually dependent processes, the liquid temperature ultimately reaches its maximum value, T^*_{avg}, when the rate of boiling heat consumption, $q_c(t)$, becomes equal to the rate of external energy deposition rate, $q_d(t)$, at $t = t^*$. After time, t^*, the external energy deposition, $q_d(t)$, is no longer sufficient to support associated bubble generation and growth. In this situation, the huge number of bubble generations and their growth are accompanied by a corresponding decrease in the liquid sensible energy, which results in an autonomous evaporation condition as indicated in Figure 5 by the sudden drop in the average liquid temperature curve after $t = t^*$. In addition, at this stage, vapor generation is assumed to be enough to occur on a massive scale that corresponds to possible boiling explosion or vapor explosion. In the present model, the criteria of boiling explosion has been defined as the onset of the loss of liquid sensible energy for the generation and growth of bubbles associated with the liquid boiling phenomena. More simply,

Table 1. Boundary conditions and solutions [49].

(1) Linearly increasing temperature	(2) High heat flux pulse heating	(3) Contact with high temperature solid
$T_w(t) = bt$	$q_w = q$	$T_i = \frac{\beta T_b + T_0}{1+\beta}$ and $\beta = \sqrt{\frac{(\rho c\lambda)_s}{(\rho c\lambda)_l}}$
$T(x,t) = T_0 + 4bti^2 erfc\left(x/\sqrt{4\alpha t}\right)$ (16)	$T(x,t) = T_0 + \frac{q\sqrt{4\alpha t}}{\lambda} ierfc\left(x/\sqrt{4\alpha t}\right)$ (17)	$T(x,t) = T_0 + (T_i - T_0) erfc\left(x/\sqrt{4\alpha t}\right)$ (18)

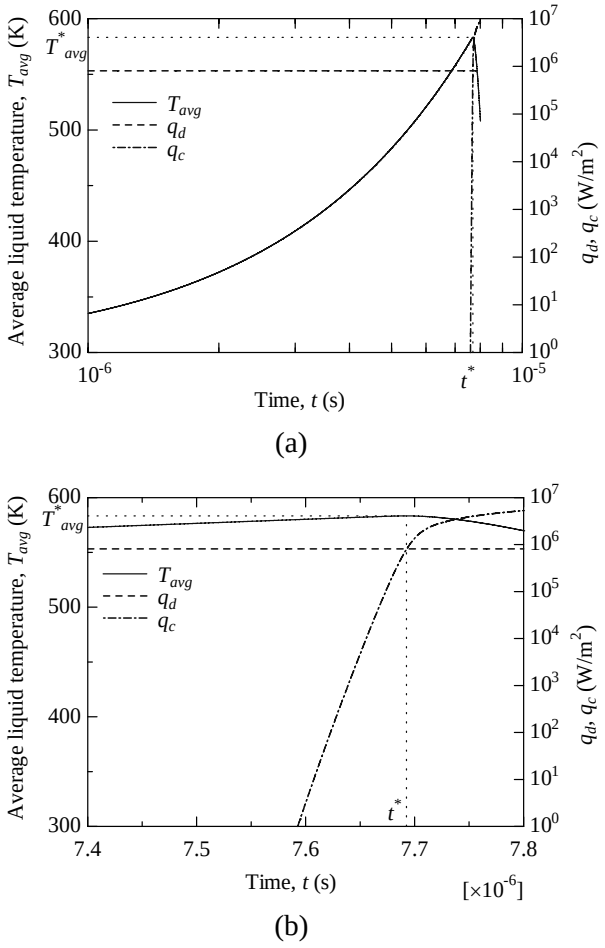

Figure 5. Temporal variation of average liquid temperature, external energy deposition rate and boiling heat consumption rate within the liquid control volume (b = 37.3×10^6 K/s and T_0 = 298.15 K).

boiling explosion is assumed to occur at time, $t = t^*$, with the maximum attainable liquid temperature, $T = T^*_{avg}$, under the following inequality of the homogeneous boiling energy consumption and the external energy deposition:

$$q_c(t) \geq q_d(t)$$

Figure 6 illustrates the time-temperature history of a finite liquid cluster for various heating rates ranging from 37.3×10^6 K/s to 1.80×10^9 K/s. As shown in Figure 6, with higher heating rates, the boiling explosion condition is obtained much earlier while maximum attainable liquid temperature is slightly increased by about 3 K within the change of b = 37.3×10^6 K/s to 1.80×10^9 K/s. The time at

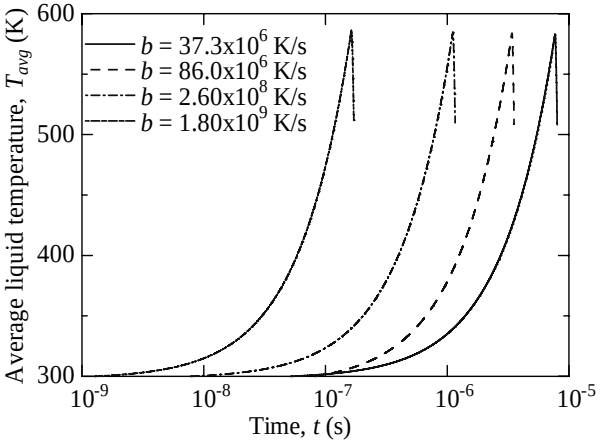

Figure 6. Temperature escalation during rapid water heating for various boundary heating rates (b).

which boiling explosion takes place, proportionally decreases with an increase in the heating rate.

For the case of pulse heating experiments, Skripov [24] recommended the threshold nucleation rate to be in the range of J = 10^{18} to 10^{28} m^{-3}s^{-1}. The iterative solution of the homogeneous nucleation rate equation for the maxima of this range of threshold nucleation rate yields a limiting liquid superheat temperature of 587 K. As shown in Figure 7, the limit of maximum attainable liquid temperature has been found to be within the range of 583-587 K, depending on the heating rate (b) that ranges from 37.3×10^6 K/s to 1.80×10^9 K/s. Note that, the nucleation rate at the time of boiling explosion as per the model prediction, corresponds to approximately 10^{23} to 10^{28} m^{-3}s^{-1}, depending on the heating rate, b.

Figure 8 depicts the boiling configurations over a small film heater at different times as observed by Iida *et al.* [29], during rapid water heating from an initial liquid temperature of 298.15 K at a heating rate of 37.3×10^6 K/s at atmospheric pressure. As shown in Figure 8, the condition of boiling explosion may be assumed to be between 7.65 μs and 7.85 μs when the entire heater surface is on the verge of being covered by a vapor blanket. In this case, the developed model predicts that the condition of boiling explosion will occur at 7.69 μs at a maximum liquid temperature of 583.3 K. Figure 9 also presents the other photographs of progressive stages of explosive vaporization of water on an ultrathin Pt wire as reported by G1od *et al.* [27]

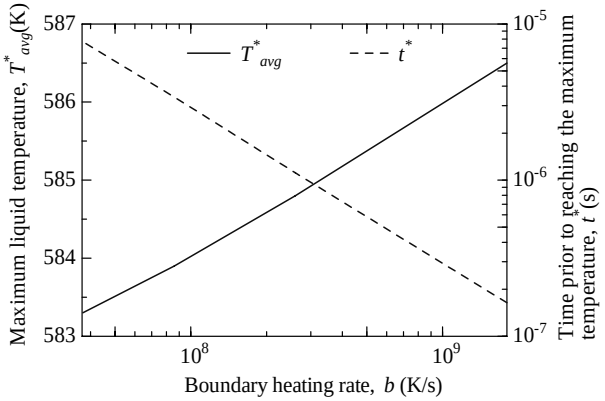

Figure 7. Effect of boundary heating rate (b) on maximum attainable liquid temperature (T^*_{avg}) and time prior to reaching the limit, i.e., boiling explosion (t^*).

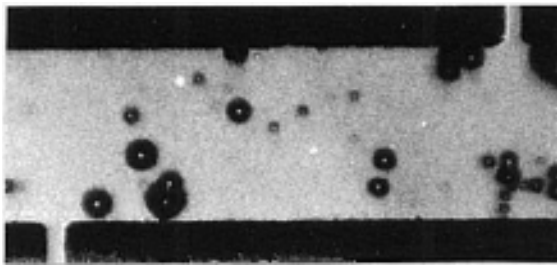

(a) t = 7.45 μs

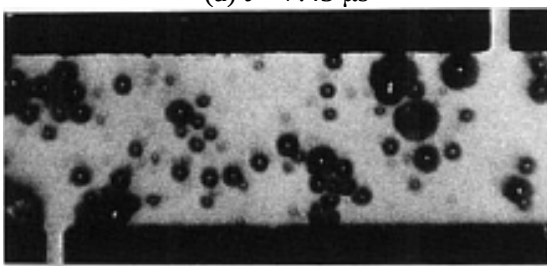

(b) t = 7.65 μs

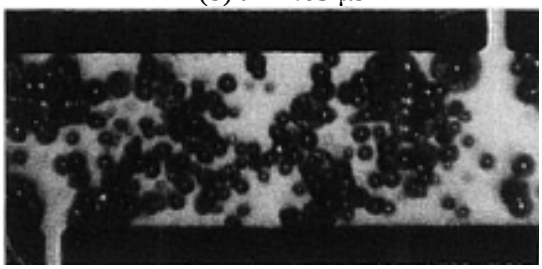

(c) t = 7.85 μs

Figure 8. Boiling configurations over a small film heater at $b = 37.3\times10^6$ K/s and T_0 = 298.15 K (Reprinted from Iida, Y., Okuyama, K. and Sakurai, K., International Journal Heat and Mass Transfer, 37(17), 2771 Copyright (1994) with permission from Elsevier); Model predicted time of boiling explosion, t^* = 7.692 μs.

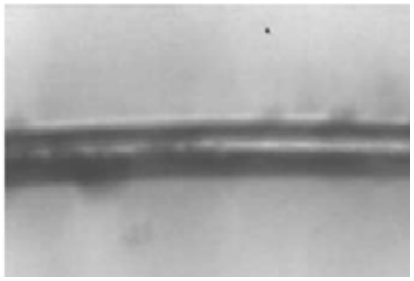

(a) t = 3.0 μs

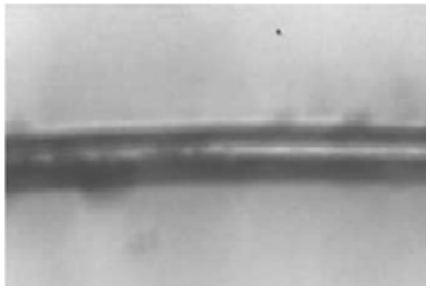

(b) t = 3.5 μs

Figure 9. Progressive stages of explosive boiling at $b = 86.0\times10^6$ K/s and T_0 = 293.15 K (Reprinted from Glod, S., Poulikakos, D., Zhao, Z. and Yadigaroglu, G., International Journal of Heat and Mass Transfer, 45, 367 Copyright (2002) with permission from Elsevier); Model predicted time of boiling explosion, t^* = 3.407 μs.

for a heating rate of $b = 86.0\times10^7$ K/s. As shown in the photographs, the wire surface is almost instantaneously covered by a thin vapor film. However, during the initial stages of vaporization, Glod *et al.* [27] pointed out "ready centers" on the wire surface that initiate and develop the boiling explosion process. As shown in Figure 9, no significant change in the liquid pattern is observed until 3 μs after the start of heating. At 3.5 μs, the liquid is found to be driven away explosively from the wire surface due to possible bubble generation and growth as observed in Figure 9(b). For the identical initial and boundary conditions of Glod *et al.* [27], the model predicts that the boiling explosion condition would occur at 3.40 μs at a maximum liquid temperature of 583.9 K.

It may be worth mentioning that at higher heating rates of 2.60×10^8 K/s and 1.80×10^9 K/s [30], the observed time at which massive tiny bubbles appear, almost corresponds to the predicted time of 1.11 and 0.163 μs, which are in agreement

Table 2. Simulation results for various boundary heating rates (b).

T_0 (K)	b (K/s)	T^*_{avg} (K)	t^* (μs)	x_e (nm)
298.15	37.3×10^6	583.3	7.692	5.21
293.15	86.0×10^6	583.9	3.407	5.11
298.15	2.60×10^8	584.8	1.114	4.97
298.15	1.80×10^9	586.5	0.163	4.71

within acceptable range, respectively. In addition to this, the corresponding maximum temperatures become 584.8 K and 586.5 K, respectively. The summary of the simulation results for various boundary heating rates (b) has been presented in Table 2.

For water heating at atmospheric pressure, the present model proposes the following approximate Eqs. for the time of the boiling explosion, t^* (μs) and the maximum attainable cluster temperature, T^*_{avg} (K) for a wide range of the boundary heating rate b (K/s) and liquid initial temperature, T_0 (K) as

$$t^* = \left[2.93 - 0.01\left(T_0 - 273\right)\right]\times10^8 b^{-0.995} \quad (19)$$

$$T^*_{avg} = 0.7\ln\left(b\right) + 571.2 \quad (20)$$

for $10^5 < b < 2\times10^9$ K/s and $273 < T_0 < 373$ K.

Note that for a particular boundary heating rate, the time of the occurrence of the boiling explosion depends on the liquid initial temperature as the nucleation occurs earlier for a higher liquid initial temperature. However, as the nucleation occurs at much higher temperature range than the liquid initial temperature, no substantial effect of the liquid initial temperature, T_0, on the maximum attainable liquid temperature, T^*_{avg}, has been found. Therefore, the maximum attainable liquid temperature, T^*_{avg} depends only on the liquid heating rate, b.

4.3. High heat flux pulse heating

Many experimental studies have been conducted by several research groups to understand the explosive boiling on microheaters immersed in liquids under the action of high heat flux pulse heating [33-39]. The solution for this case has already been listed in Table 1.

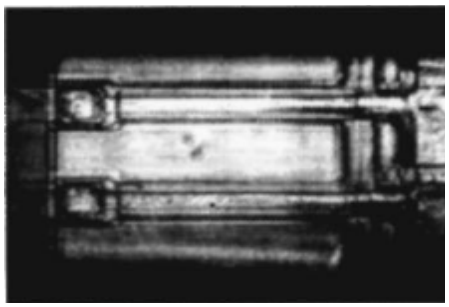

(a) t = 2.1 μs

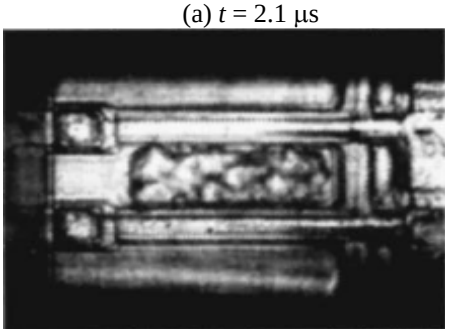

(b) t = 3.0 μs

Figure 10. Experimental observation of boiling explosion in water at (q = 265 MW/m^2, T_0 = 293 K) (Reproduced from Hong, Y., Ashgriz, N. and Andrews, J. 2004, ASME Journal of Heat Transfer, 126, 259 with permission from ASME); model predicted time for boiling explosion: t^* = 2.39 μs.

For this type of liquid heating case, the initial and boundary conditions identical to that of Asai [34] are chosen that corresponds to a boundary heat flux, q = 100 MW/m^2 with a liquid initial temperature, T_0 = 298 K. For this initial and boundary conditions, the present model predicts the boiling explosion (i.e., $q_c(t) = q_d(t)$ and $dT_{avg}/dt = 0$) to be at t^* = 15.98 μs at the maximum cluster temperature, T^*_{avg} = 582.26 K while the model proposed by Asai [34] predicts the boiling explosion to be at a time of about 19.5 μs. Moreover, Asai [34] mentioned the homogeneous nucleation to occur within 5 nm of the heating surface to the ink liquid under the typical operating conditions of a bubble jet printer (q = 100 MW/m^2) which is almost the same as the liquid cluster size considered in the present model (5.39 nm). Figure 10 illustrates the progressive stages of boiling explosion in water observed during pulse heating experiments with q = 265 MW/m^2 and T_0 = 293 K conducted by Hong *et al.* [38] together with the predicted time, t^* = 2.39 μs.

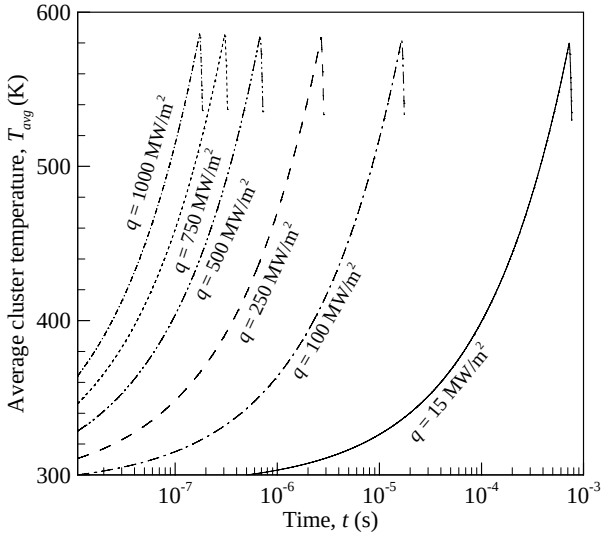

Figure 11. Temperature rise inside a characteristic liquid cluster for various heat fluxes (T_0 = 293 K).

For this case, the maximum cluster temperature is predicted to be T^*_{avg} = 583.6 K. On comparing the predicted time with the time of 2.1 μs at which the first bubble was observed, it was noticed that at t = 3.0 μs, a massive vapor is observed on the heater and the predicted time is significantly earlier than the time of 3.0 μs. This time difference might be due to small amounts of heat being dissipated into the backside of the heater during the heating process. As depicted in Figure 10, the model prediction concerning the boiling explosion is found to be in good agreement with experiments. It should be mentioned that the similar agreement can be obtained for other heat fluxes of q = 253 MW/m^2 and 453 MW/m^2 for which the predicted times become t^* = 2.64 μs and t^* = 0.98 μs, respectively.

Figure 11 shows the temperature rise inside the cluster during water heating with various heat fluxes, q, from a liquid initial temperature, T_0 = 293 K. As depicted in Figure 11, the occurrence of the boiling explosion takes place much earlier at higher heat fluxes. The minimum heat flux necessary for the occurrence of the boiling explosion is important from some practical points of view. Note that, to determine the limiting heat flux for boiling explosion, a characteristic time period of 1 millisecond for the occurrence of the boiling explosion has been considered in the present study. Beyond this characteristic time period, heterogeneous nucleation might play the key role for boiling incipience. As shown in Figure 11, the value of the minimum heat flux for water corresponds to about 15 MW/m^2. Asai [34] also mentioned the minimum heat flux or the threshold heat flux to be in order of 100 MW/m^2 for reproducible and powerful bubble generation processes. As pointed out by Asai [34], the nucleation process becomes more random for heat fluxes lower than the threshold limit. This randomness in the nucleation process might be due to the heterogeneous nucleation which might take place after 1 millisecond from the commencement of heating process as considered in the present model. The apparent difference between the limiting heat fluxes for boiling explosion reported by Asai [34] and as obtained in the present model might be due to various unexpected factors involved in the experimentations. However, this difference might be considered acceptable from engineering point of view. Zhao *et al*. [50] have also mentioned the criteria for minimum heat flux for explosive boiling to occur on the basis of maximum possible heat flux across the liquid-vapor interface, $q_{max,.max}$. For water at atmospheric pressure, they speculated a minimum heat flux of 224 MW/m^2 to be required for explosive boiling.

As shown in Figure 11, the time of the boiling explosion strongly depends on the heat flux, q. For instance, a variation of about two orders in the magnitude of the heat flux, q, (15-1000 MW/m^2) has been found to result in a variation of about three orders in the magnitude of the boiling explosion time, t^*, (0.723 ms-0.173 μs). A similar trend of the variation of the boiling explosion time, t^*, with heat flux, q, has been obtained for the liquid initial temperatures, T_0, ranging from 293 K to 373 K. The present model proposes the following approximate Eq. (21) for the time of the boiling explosion, t^* (μs), for water heating at atmospheric pressure as a function of the heat flux, q (MW/m^2) and liquid initial temperature, T_0 (K):

$$t^* = \left[1.71 - 0.01\left(T_0 - 273\right)\right] \times 10^5 \, q^{-1.98} \qquad (21)$$

for 15 < q < 1000 MW/m^2 and 293 < T_0 < 373 K.

Contrary to the time of the boiling explosion t^*, the maximum cluster temperature, T^*_{avg}, that is the liquid temperature at the boiling explosion did not change much with the variation in the heat flux. However, the liquid penetrates deeper in the metastable region prior to the boiling explosion during heating with higher heat fluxes. In the present study, for a variation of the heat flux, q, from 15 MW/m^2 to 1000 MW/m^2, the maximum attainable cluster temperature, T^*_{avg}, has been found to increases about 6 K only (580-586 K). However, no substantial effect of the liquid initial temperature, T_0, on the maximum attainable liquid temperature, T^*_{avg}, has been found. Therefore, the variation of the maximum attainable liquid temperature, T^*_{avg} (K) at the boiling explosion has been expressed as a function of the heat flux, q (MW/m^2) only as Eq. (22).

$$T^*_{avg} = 1.43\ln(q) + 575.9 \qquad (22)$$

for $15 < q < 1000$ MW/m^2

Note that the temperature limit at the boiling explosion obtained in the present study for water at atmospheric pressure has been found to be in good agreement with the limiting superheating temperature obtained by Varlamov *et al.* [37] for pulse heating conditions (587 K).

4.4. Contact with high temperature solid

Liquid interaction in contact with preheated solid surface (spray cooling, jet cooling, fire fighting) may result in homogeneous boiling explosion depending on the pre-contact temperatures of the solid and the liquid and their thermo-physical properties. For more clarification, the experimental observation made by Woodfield *et al.* [8] during jet impingement quenching of high temperature surface as shown in Figure 12 might be referred herein. Figure 12 shows a typical cooling curve and recorded audible sound obtained by Woodfield *et al.* [8] during jet impingement quenching. As the authors [8] explained, the first strong sound could be heard as a sharp spattering sound and a repetition of wet and dry surface conditions takes place at very short periods. Note that the wet surface condition mentioned here refers to the surface condition during direct solid-liquid contact while dry surface condition refers to that after boiling explosion that might occur due to rapid liquid heating during brief solid-liquid contact. It is interesting that during the repetition of wet and dry surface conditions, the measured thermocouple does not show any change because a short period change in surface temperature does not penetrate to the thermocouple sensor location. On closer observation at the early stages of jet impingement quenching, Islam *et al.* [9] found a chronological change in liquid flow patterns over the surface depending on the surface temperature. They observed a chaotic flow pattern when the surface temperature remains above a certain limit, T_{limit}, while a calm sheet-like flow pattern was found as the surface cools down below T_{limit}. The limiting surface temperature, T_{limit}, has been defined by the authors with the presumption of jet impingement on a solid surface as a two semi-infinite body contact problem with a constant thermodynamic superheat limit of the liquid, T_{TSL} (as assumed to be 312°C for water at atmospheric pressure). The analytical expression of T_{limit}, the pre-contact liquid jet temperature (T_0), the limit of maximum liquid superheat (T_{TSL}) and the thermo-physical properties of the solid block and the liquid jet can be given as follows as mentioned in [49]:

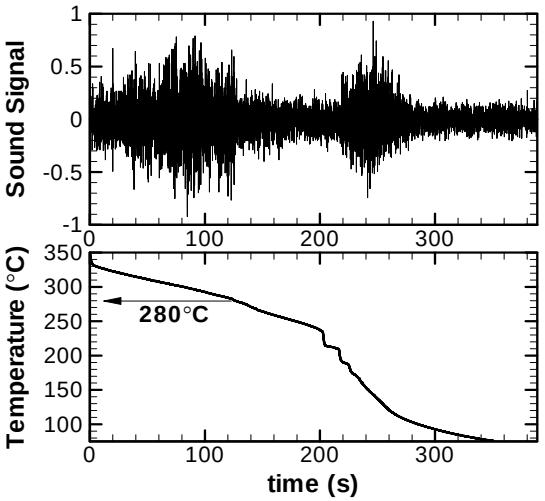

Figure 12. Audible sound during quench (embedded thermocouple reading: 4 mm from center and 5 mm beneath the surface; Mat.: Cu, T_b = 350°C; Water jet: u_j = 3 m/s, T_0 = 49°C) (Reprinted from Woodfield, P. L., Monde, M. and Mozumder, A. K., International Journal of Heat and Mass Transfer, 48, 2032 Copyright (2005) with permission from Elsevier).

$$\frac{T_{\lim it} - T_{TSL}}{T_{TSL} - T_0} = \frac{1}{\beta} = \sqrt{\frac{(\rho c \lambda)_l}{(\rho c \lambda)_s}} \quad (23)$$

Islam *et al.* [9] speculated that unstable film boiling or explosive boiling might be the possible heat transfer mode in the early stages of jet impingement quenching; some brief solid-liquid contact makes the surface wet and cool while the subsequent boiling explosion makes the surface again dry during which surface temperature recovers due to heat conduction inside the solid. With the repetition of wet and dry surface condition, the surface ultimately cools down below a certain limit (T_{limit}) that allows stable solid liquid contact without any boiling explosion. To apply the present model of homogeneous nucleation boiling explosion to the case of liquid heating that occurs during brief solid-liquid contact, the heat transfer process has been considered as a two semi-infinite solid contact problem. With this assumption, the solution for this case can be obtained as given by Eq. (18) in Table 1.

Figure 13 depicts the temporal variation of the average cluster temperature, T_{avg}, within a finite liquid cluster at the solid-liquid boundary when a water jet (20°C) comes in contact with hot steel surface at various temperatures (335-550°C). As shown in Figure 13, in the case of liquid contact with higher temperature surface, the liquid is heated up to a much higher temperature prior to the attainment of the boiling explosion condition ($dT_{avg}/dt = 0$) and also the time necessary to attain the boiling explosion condition, t^*, decreases sharply. Note that for the special case of surface temperature, T_b = 335°C, the liquid temperature asymptotically approaches the interface temperature without attainment of the boiling explosion condition within 1 ms. This phenomenon points out that for solid temperatures at or below 335°C with all other quench conditions being the same, the vapor generation during direct solid-liquid contact is not high enough to hinder stable solid-liquid contact. In other words, the flow patterns corresponding to the surface temperature at or below 335°C would be calm and quiet as stable solid-liquid contact is established in these conditions. For solid surfaces, at a temperature higher than 335°C, boiling explosion in the cluster

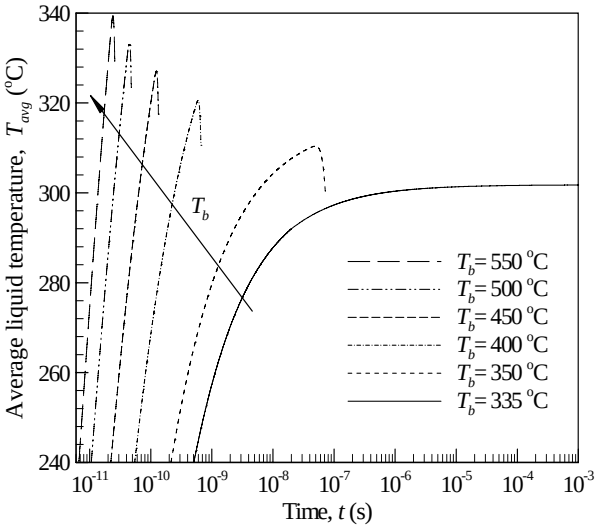

Figure 13. Average liquid temperature escalation inside the liquid cluster during contact of a water jet (20°C) with steel surface at various temperatures (335-550°C).

will result in the unstable repetition of wet and dry surface condition, and therefore chaotic flow patterns prevail until its temperature is cooled down below 335°C in a fashion similar to that obtained by Woodfield *et al.* [8] as depicted in Figure 12. Moreover, Woodfield *et al.* [8] reported the calm and quiet flow condition with steady solid-liquid contact to occur at a surface temperature of 280°C as shown in Figure 12. Results predicted by the present model differ from that of Woodfield *et al.* [8] due to the variation of quench conditions (solid-liquid combination and liquid initial temperature) between these two cases under consideration. However, the limiting condition of steady solid-liquid contact in both cases can be compared in terms of the corresponding interface temperature, T_i. According to the present model, there is no boiling explosion due to homogeneous nucleation boiling at a solid surface temperature of 335°C with a corresponding interface temperature of 303°C. The interface temperature for the Woodfield *et al.* experiment [8] becomes 337°C at the moment of the first liquid contact with the solid. After repetitions of solid-liquid contact, the surface temperature goes down to 280°C at which the interface temperature assumes a value of about 270°C. Considering 303°C as the limiting interface boundary temperature for the occurrence of the boiling explosion due to homogeneous

nucleation only, the observed explosive liquid flow pattern and the recorded high pitch sound in Woodfield's experiment [8] might be due to homogeneous nucleation boiling for the surface temperatures ranging from 350°C to 314°C (corresponding to the interface temperature 303°C for the given solid-liquid combination and their pre-contact temperatures) while that might be due to heterogeneous nucleation boiling for the surface temperatures ranging from 314°C to 280°C.

The effect of solid surface temperature on the characteristics of homogeneous nucleation boiling explosion phenomena has been manifested in Table 3. As mentioned in Table 3, the limit of maximum attainable liquid temperature increases over 30°C for an increase of 200°C in the solid surface temperature while the time of boiling explosion decreases about two orders of magnitude for the same variation. The size of the liquid cluster under the consideration also decreases with the increase in the solid surface temperature.

5. Lower limit of homogeneous nucleation boiling explosion in water

The limiting condition for boiling explosion due to homogeneous nucleation is very important for better design and control of various thermal micromachines based on the principle of explosive boiling. This is also important for the prediction of the onset of stable wetting during liquid contact with hot surfaces as in the case of jet impingement quenching or spray quenching. In order to determine the lower limit for the occurrence of homogeneous nucleation boiling explosion in water at atmospheric pressure, the present model has been adopted with two different boundary conditions, namely, linearly increasing temperature condition and constant temperature condition.

5.1. Liquid heating with linearly increasing temperature

This condition essentially describes the pulse heating technique and droplet superheat technique in the bubble column. These two techniques have been frequently applied to determine experimentally the liquid superheat limit. In the present study, the heating rate has been considered to vary from 10 K/s to 10^9 K/s. The upper limit of this range includes the typical heating rate used in pulse heating experiments [27, 29, 30] while the lower limit corresponds to a typical droplet superheating condition [51]. Figure 14 depicts the temperature rise inside the cluster and also the occurrence of homogeneous boiling explosion for various boundary heating rates with the initial liquid temperature, T_0 = 20°C. As shown in Figure 14, the boiling explosion condition, i.e., the onset of the decrease of average cluster temperature due to bubble nucleation and growth, takes place earlier for higher heating rates. The summary of simulations has been presented in Table 4. As mentioned in Table 4, the size of cluster under the consideration gradually decreases for higher rates of heating. As shown in Table 4, for a variation of eight orders of magnitude in the heating rate the maximum attainable temperature at which homogenous boiling explosion occurs, increases about 11°C only while the corresponding time of homogeneous boiling explosion changes roughly by eight orders of magnitude.

It is interesting that, the nucleation rates, J ($m^{-3}s^{-1}$), at the boiling explosion for different heating rates

Table 3. Simulation results for quenching of carbon steel surface (350-500°C) with water jet (20°C) at atmospheric pressure.

T_0 (°C)	T_b (°C)	T_i (°C)	x_e (nm)	T^*_{avg} (°C)	t^* (ns)
20	350	316.5	5.17	310.4	49.68
	400	361.4	3.71	320.5	0.595
	450	406.3	2.96	327.1	0.123
	500	451.3	2.41	333.4	0.044
	550	496.2	2.40	339.3	0.024

as obtained in the present model study are of similar order of "threshold nucleation" rates for different liquid superheating techniques as mentioned in Ref. [22]. For instance, a threshold nucleation rate of $J = 10^{12}$ - 10^{13} $m^{-3}s^{-1}$ and $J = 10^{24}$ - 10^{29} $m^{-3}s^{-1}$, is considered for typical droplet superheat experiment and pulse heating experiment respectively [22]. However, the nucleation rate at the boiling explosion as per the present model corresponds to a value of $J = 10^{7}$ $m^{-3}s^{-1}$ and $J = 10^{26}$ $m^{-3}s^{-1}$ for a representative droplet superheating experiment (b = 10 K/s) and pulse heating experiment ($b = 10^{9}$ K/s), respectively. For better understanding, one might be interested in the number of bubbles generated in the cluster prior to the boiling explosion, J^* ($1/m^2$), that has been defined as

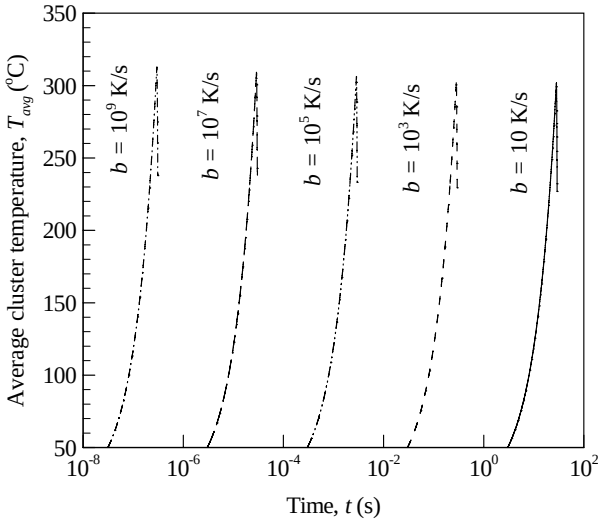

Figure 14. Temperature escalation inside a characteristic liquid cluster for various heating rates (T_0 = 20°C).

$$J^* = x_e \int_0^{t^*} J(t)dt \tag{24}$$

As mentioned in Table 4, J^* increases sharply with the heating rate. For the case of b = 10 K/s, J^* is obtained to be less than unity. This is due to the fact that the cluster in the liquid can appear in any location as the temperature in the liquid is raised almost uniformly. Therefore, one should consider larger liquid volume in place of x_e in which boiling explosion might occur.

5.2. Liquid heating with constant temperature condition

The heat transfer process between a solid and a contacting liquid can be assumed to be a two 1-D semi-infinite body contact problem, liquid with a constant interface temperature, T_i, determined by the initial liquid temperature, the solid temperature and the thermo-physical properties of the solid-liquid combination through a parameter as β.

The temperature rise inside the cluster during water (20°C) contact with hot steel surfaces (335-340°C) at atmospheric pressure is shown in Figure 15. As shown in this figure, during contact with higher temperature surfaces, the condition of homogeneous nucleation boiling explosion appears much earlier with a relatively higher cluster temperature. For the case of liquid contact with the surface at 335°C, the condition of homogeneous boiling explosion does not occur within a time period of 1 millisecond. After this characteristic time period, heterogeneous nucleation boiling might play the key role for vaporization. The summary of simulation results is listed in Table 5. From this table, it is evident that boiling explosion over hot steel surface occurs within a characteristic time period of about 1 millisecond, for a surface

Table 4. Homogeneous nucleation characteristics at various heating rates (b).

T_0 (°C)	b (K/s)	x_e (nm)	T^*_{avg} (°C)	t^* (s)	J^* ($1/m^2$)
20	10	6.72	301.8	2.82×10^{1}	0.007
	10^3	6.32	303.9	2.84×10^{-1}	6.17
	10^5	5.88	306.3	2.87×10^{-3}	5.19×10^{3}
	10^7	5.38	309.2	2.90×10^{-5}	4.20×10^{6}
	10^9	4.79	312.8	2.97×10^{-7}	3.07×10^{9}

temperature at or above 336°C for water contact with an initial water temperature of 20°C at atmospheric pressure. This lower limiting condition of homogeneous boiling explosion corresponds to a maximum liquid temperature of about 303°C at the boiling explosion with a limiting interface temperature of around 304°C. Also note that the number of bubbles generated in the cluster prior to the boiling explosion, J^*, depends much on the surface temperature. During contact with lower temperature surface, slow and steady liquid heating might result in clusters/bubbles beyond the cluster thickness as in the extremely slow heating case (b = 10 K/s) as discussed in Sec. 5.1.

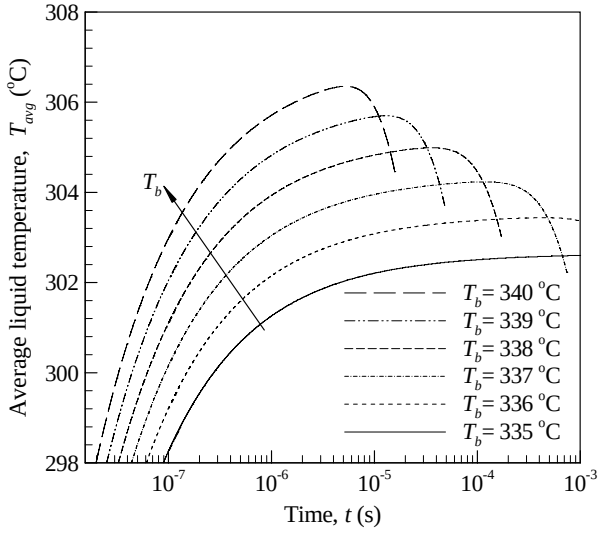

Figure 15. Temperature escalation inside a characteristic liquid cluster during water contact with hot steel surfaces (β = 8.86, T_0 = 20°C).

As found in the present study, for a particular liquid initial temperature and particular solid-liquid combination, there exists a limiting surface temperature say, T^*_b, below which no homogeneous nucleation boiling explosion occurs. The variation of this limiting surface temperature with the liquid initial temperature has been tabulated in Table 6 for contact of water with hot steel surface. Theoretically, the limiting interface temperature as well as the liquid temperature in the cluster at the boiling explosion should be the same for all combinations of T_0 and T^*_b. However, as a margin of 1°C has been allowed in defining the limiting surface temperature for homogeneous boiling explosion (T^*_b) some variations occurred in the corresponding limiting interface temperature (T^*_i) as well as in the maximum attainable cluster temperature (T^*_{avg}) for different combinations of T_0 and T^*_b as mentioned in Table 6. However, with an average interface temperature, T^*_i = 304°C for all combinations of T_0 and T^*_b, the condition of homogeneous boiling explosion has been found to occur around a maximum attainable cluster temperature, T^*_{avg} = 303°C, within a time period of about 0.5 millisecond after contact. Note that the temperature limit obtained for this case of liquid heating is also close to the temperature limit at which homogeneous boiling explosion occurs during slow and steady heating with a linearly increasing temperature condition (b = 10 K/s). Moreover, this temperature limit at the homogeneous boiling explosion is the same as that predicted by Lienhard's [18] correlation for homogeneous nucleation in water at atmospheric pressure. With the pre-assumption of the liquid-solid contact problem as a two 1-D semi-infinite

Table 5. Homogeneous nucleation characteristics during liquid contact with hot steel surface at various temperatures (β = 8.86).

T_0 (°C)	T_b (°C)	T_i (°C)	x_e (nm)	T^*_{avg} (°C)	t^* (μs)	J^* (1/m^2)
20	335	303.0	6.55	-	-	-
	336	303.9	6.41	303.4	443.46	0.48
	337	304.8	6.26	304.2	117.42	6.90
	338	305.7	6.12	305.0	36.11	7.36×10^{1}
	339	306.6	5.99	305.7	12.85	5.92×10^{2}
	340	307.5	5.87	306.3	5.239	3.67×10^{3}

Table 6. Limiting condition of homogeneous nucleation boiling over hot surface [$\beta = 8.86$] during liquid contact at various temperatures.

T_0 (°C)	T^*_b (°C)	T^*_i (°C)	x_e (nm)	T^*_{avg} (°C)	t^* (s)
0	338	303.7	6.45	303.2	5.3×10^{-4}
20	336	303.9	6.41	303.4	
40	334	304.2	6.36	303.6	
60	331	303.5	6.47	303.1	
80	329	303.7	6.42	303.3	
100	327	304.0	6.38	303.6	

Table 7. Limiting surface temperature for homogeneous nucleation boiling during water contact with various hot surfaces.

T^*_i (°C)	β	T_0 (°C)	T^*_b (°C)
304	8.86	0-100	338-327
	11.06		331-322
	22.63		317-313

body contact problem, once the limiting interface temperature for homogeneous boiling explosion is known, it is possible to determine the limiting surface temperature for liquid contact with any other solid surfaces readily from the definition of the interface temperature as follows:

$$T_b^* = T_i^* + \frac{1}{\beta}\left(T_i^* - T_0\right) \tag{25}$$

The variation of the limiting surface temperature, T^*_b, for homogeneous boiling explosion during water contact with steel ($\beta = 8.86$), brass ($\beta = 11.06$) and copper ($\beta = 22.63$) has been tabulated in Table 7 for various liquid initial temperatures ranging from 0°C to 100°C for a limiting interface temperature of homogeneous boiling explosion, T^*_i = 304°C. The inter-dependency among T^*_b, T_0 and β presents a boundary surface in a T_b–T_0–β co-ordinate system as shown in Figure 16 above which boiling explosion due to homogeneous nucleation occurs instantaneously and below which it does not.

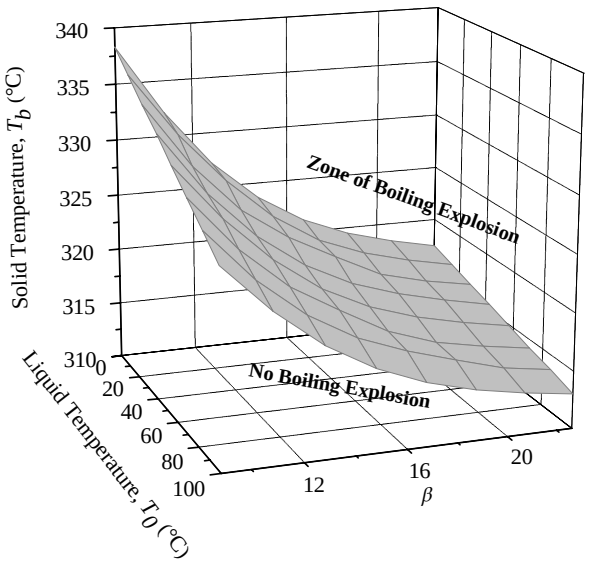

Figure 16. Boundary for homogeneous boiling explosion on $T_b - T_0 - \beta$ plane.

6. Comparison between attainable maximum heat flux with upper bound of maximum heat flux and continuum characteristics

The boiling explosion condition as defined in the present model might be compared with the theoretical explosion condition in terms of the maximum possible heat flux across the liquid-vapor interface, $q_{max,max}$. As proposed by Gambill and Lienhard [53], the maximum possible heat flux across the liquid-vapor interface, $q_{max,max}$, that can be conceivably achieved in a vaporization or condensation process can be expressed as follows:

Table 8. Heat flux across the liquid-vapor interface, $q^*_{l\text{-}v}$, and $q_{max,max}$ and number of molecules inside the critical vapor embryo (N) at the boiling explosion ($t = t^*$) for various heating rates (b).

T_0 (K)	b (K/s)	$q^*_{l\text{-}v}$ (W/m^2)	$q_{max,\,max}$ (W/m^2)	N
298.15	37.3×10^6	7.22×10^9	1.49×10^{10}	135
293.15	86.0×10^6	7.31×10^9	1.50×10^{10}	128
298.15	2.60×10^8	7.44×10^9	1.52×10^{10}	120
298.15	1.80×10^9	7.71×10^9	1.55×10^{10}	105

$$q_{\max,\max} = \rho_v L\sqrt{RT/2\pi} \tag{26}$$

The heat flux across the liquid-vapor interface of a bubble $q_{l\text{-}v}$, can be obtained as

$$q_{l-v} = \rho_v L\frac{dr}{dt} \tag{27}$$

If $q^*_{l\text{-}v}$ corresponds to the heat flux across the liquid-vapor interface of a bubble at the time of boiling explosion, $t = t^*$, then

$$q^*_{l-v} = \rho_v L\frac{dr}{dt}\Big|_{t=t^*} \tag{28}$$

Bubbles of different sizes co-exist at $t = t^*$. Therefore, the individual bubble has its own growth rate depending on its lifetime; that is the bubble grows at the different heat flux across the liquid-vapor interface. We choose the largest heat flux at the interface of the bubble which is generated just before the boiling explosion, namely, at the time $t = t^*$. Near the time $t = t^*$, the growth of this bubble is essentially controlled by the inertia and to calculate the heat flux $q^*_{l\text{-}v}$, with the consideration of inertia controlled bubble growth, we adopted the bubble growth model proposed by Rayleigh [54].

Table 8 summarizes the heat flux characteristics across the liquid-vapor interface of the bubble and also the number of molecules in the cluster at the boiling explosion for various linearly increasing temperature cases. As shown in this table, the largest heat flux $q^*_{l\text{-}v}$, is lower than the maximum limit $q_{max,max}$, for all values of heating rates considered therein. This is due to the fact that the limit of maximum possible heat flux $q_{max,max}$, is obtained with the unique assumption of no condensation at the liquid-vapor interface. In reality, there would be some condensation in parallel with the vaporization during the bubble growth. It is important to justify the length scale of the critical vapor embryo (i.e., $2r_c$) which has been considered as the size of cluster (x_e) in the present model for the application of macroscopic property values, such as surface tension and density. As continuum characteristics, the number of molecules within a critical bubble at the time of boiling explosion has been considered. It has been found that the number of molecules within the vapor embryo at the time of boiling explosion exceeds 100 for all values of heating rates under consideration as mentioned in Table 8.

For the contact with a lower temperature solid surface, the heat flux across the liquid-vapor interface at the time of boiling explosion $q^*_{l\text{-}v}$, is lower than the maximum limit $q_{max,max}$, as mentioned in Table 9. However, for the cases with a higher temperature solid surface, $q^*_{l\text{-}v}$ ultimately approaches $q_{max,max}$. This variation of $q^*_{l\text{-}v}$ with the surface temperature simply points out that, during contact of a liquid with very hot surface, the boiling explosion occurs almost instantaneously resembling the hypothetical condition of "no return of vapor molecules" at the liquid-vapor interface as assumed by Gambill and Lienhard [54]. In addition, from Table 9 it may be noted that, at a solid block temperature beyond about 550°C, the boiling explosion may occur at the heat flux $q_{max,max}$, because $q^*_{l\text{-}v}$ never becomes larger than $q_{max,max}$. As mentioned in [55], continuum consideration may be applicable for liquid thickness over 10 molecular layers. Therefore,

Table 9. Heat flux across the vapor interface ($q^*_{l\text{-}v}$) and limit of maximum heat flux "$q_{max,max}$" at $t = t^*$ for water (20°C) contact with hot steel surfaces (350-550°C) at various temperatures and the number of molecules in the critical vapor embryo.

T_b (°C)	t^* (ns)	$q^*_{l\text{-}v}$ (W/m^2)	$q_{max,\,max}$ (W/m^2)	N
350	49.68	7.25×10^{9}	1.50×10^{10}	133
400	0.595	9.05×10^{9}	1.68×10^{10}	59
450	0.123	1.09×10^{10}	1.81×10^{10}	34
500	0.044	1.47×10^{10}	1.92×10^{10}	21
550	0.024	2.26×10^{10}	2.01×10^{10}	20

with the presence of about 20 molecules in the critical bubble, it has been assumed that the continuum characteristic has been satisfied.

CONCLUSION

The main outcomes of the present research can be summarized as follows:

(1) A new theoretical model based on the idea of 1-D heat conduction and the theory of homogeneous nucleation boiling has been developed to study the boiling explosion phenomena.

(2) An appropriate size of liquid layer known as the characteristic liquid cluster has been proposed for non-equilibrium practical liquid heating conditions.

(3) While boiling explosion had been defined arbitrarily in earlier research, a particular stage of liquid heating has been defined as the boiling explosion in the present study, that is, the onset of decrease of liquid sensible energy due to massive scale vaporization.

(4) The condition of the boiling explosion defined in the present model has been found to be in good agreement with experimental microscale boiling explosion.

(5) The variation of liquid flow patterns observed in early stages of jet impingement quenching is due to the occurrence of homogeneous boiling explosion.

(6) In the case of jet impingement quenching, the time needed for the occurrence of boiling explosion depends strongly on the surface temperature and may vary from fraction of a millisecond to that of a nanosecond.

(7) The longest time scale for the homogeneous boiling explosion to occur during jet impingement quenching or by any other liquid heating condition might be considered to be in the order of 1 millisecond.

(8) For water at atmospheric pressure, the temperature limit at the boiling explosion corresponds to a value of about 303°C in any liquid heating condition.

(9) The limiting interface temperature for water contact with any hot surface as obtained in the present study corresponds to about 304°C. For the cases with solid-liquid temperature higher than 304°C, instantaneous boiling explosion will hinder direct solid-liquid contact. Therefore, no stable wetting is possible for water jet impingement as long as the surface temperature is cooled down enough to have solid-liquid temperature lower than 304°C.

(10) For linear heating of water, the heating rate should be higher than 10^6 K/s for homogeneous boiling explosion while for water heating with high heat flux heating, this condition corresponds to a heat flux of 1.5×10^6 W/m^2.

ACKNOWLEDGEMENT

The present study has been supported by Grant-in-aid for Scientific Research (B) 20360101, 2008 and Scientific Research (C) 24560238, 2012. The authors would like to appreciate Professor K. Okuyama of Yokohama National University, Japan and D. Poulikakos of Swiss Federal Institute of technology, Switzerland, for offering the valuable photos and helpful discussion.

SYMBOLIC TERMS

a	Thermal diffusivity	m^2/s
b	Rate of boundary temperature rise	K /s
c	Specific heat	kJ/(kgK)
J	Rate of homogeneous nucleation events	$1/(m^3s)$
J^*	Number of bubbles generated in the cluster (x_e) at $t = t^*$	$(1/m^2)$
M	Molecular weight	kg/(kmol)
P_o	Bulk liquid pressure	Pa
P_s	Saturation pressure	Pa
q	Boundary heat flux	W/m^2
q_{in}	Incoming heat flux to the cluster at $x = 0$	W/m^2
q_{out}	Outgoing heat flux from the cluster at $x = x_e$	W/m^2
q_d	Rate of energy deposition to the liquid cluster	W/m^2
q_c	Rate of boiling heat consumption in the liquid cluster	W/m^2
$q_{l\text{-}v}$	Heat flux across the liquid vapor interface	W/m^2
$q^*_{l\text{-}v}$	Heat flux across the liquid vapor interface at $t = t^*$	W/m^2
$q_{max,,}$ $_{max}$	Theoretical upper limit of evaporative heat flux across the liquid vapor interface	W/m^2
r	Bubble radius	m
r_c	Radius of the critical vapor embryo	m
R	Universal gas constant	J/(kgK)
t	Time	s
t'	Time of bubble generation	s
t^*	Time of the boiling explosion	s
T	Temperature	K or °C
T_{avg}	Average temperature in the liquid cluster	K or °C
T^*_{avg}	Maximum attainable cluster temperature	K or °C
T_b	Solid surface temperature	°C
T^*_b	Limiting surface temperature for homogeneous boiling explosion	°C
T_i	Interface temperature	°C
T^*_i	Limiting interface temperature for homogeneous boiling explosion	°C
T_0	Liquid initial temperature	K or °C
x	Distance from the boundary	m
x_e	Size of the liquid cluster ($2r_c$)	m

Greek

λ	Thermal conductivity	W/(mK)
σ	Surface tension	N/m
ρ	Density	kg/m^3
Γ	Rate of vapor generation per unit mixture volume	$kg/(m^3s)$

Subscripts

l	Liquid
s	Solid
v	Vapor

REFERENCES

1. Schick, P. E. and Grace, T. M. 1982, Institute of Paper Chemistry: Appleton, Wisconsin Project No. 3473-2.
2. Reid, R. C. 1976, Amer. Sci., 64, 146.
3. Hess, P. D. and Brondyke, K. J. 1969, Met. Prog., 95, 93.
4. Reid, R. C. 1983, Adv. Chem. Eng., 12, 105.
5. Burgess, D. S., Murphy, J. N. and Zabetakis, M. G. 1970, U.S Bureau of Mines Rep. Invest., No. 7448.
6. Burgess, D. S., Biordi, J. and Murphy, J., 1972, U.S Bureau of Mines, PMSRC Rep. No. 4177.
7. Cronenberg, A. W. 1980, Nucl. Safety, 21, 19.

8. Woodfield, P. L., Monde, M. and Mozumder, A. K. 2005, International Journal of Heat and Mass Transfer, 48, 2032.
9. Islam, M. A., Monde, M., Woodfield, P. L. and Mitsutake, Y. 2008, International Journal of Heat and Mass Transfer, 51, 1226.
10. Asai, A. 1989, Jpn. J. Applied Physics, 28, 909.
11. Gad-el-Hak, M. 2002, The MEMS handbook, CRC Press, Boca Raton.
12. Staples, M., Daniel, K., Cima, M. J. and Langer, R. 2006, Pharma. Res., 23, 847.
13. Laser, D. J. and Santiago, J. G. 2004, J. Micromech. Microeng., 14, 35.
14. Lee, Y. K., Yi, U. C., Tseng, F. G., Kim, C. J. and Ho, C. M. 1999, Proceedings of MEMS, ASME International Mechanical Engineering, Nashville, Tennessee, USA, 419.
15. Maurya, D. K., Das, S. and Lahiri, S. K. 2005, J. Micromech. Microeng., 15, 966.
16. Eberhart, J. G. 1976, Journal of Colloid and Interface Science, 56(2), 262.
17. Spiegler, P., Hopenfeld, J., Silberberg, M., Bumpus, C. F. Jr. and Norman, A. 1963, International Journal of Heat and Mass Transfer, 6, 987.
18. Lienhard, J. H. 1984, Journal of Heat Transfer, 104, 379.
19. Volmer, M. and Webber, A. 1926, Z. Phys. Chem., 119, 277.
20. Doring, W. 1937, Z. Phys. Chem., 36, 371.
21. Blander, M. and Katz, J. L. 1975, AIChE Journal, 21(5), 833.
22. Cole, R. 1974, Advances in Heat Transfer, Academic Press, 10, 86.
23. Carey, V. P. 1994, Liquid-Vapor Phase Change Phenomena, Hemisphere Publishing Corporation.
24. Skripov, V. P. 1974, Metastable Liquids, Wiley, New York.
25. Skripov, V. P. and Pavlov, P. A. 1970, High Temperature (USSR), 8, 782-787, 833-839.
26. Derewnicki, K. P. 1985, International Journal of Heat and Mass Transfer, 28, 2085.
27. Glod, S., Poulikakos, D., Zhao, Z. and Yadigaroglu, G. 2002, International Journal of Heat and Mass Transfer, 45, 367.
28. Iida, Y., Okuyama, K. and Sakurai, K. 1993, International Journal Heat and Mass Transfer, 36(10), 2699.
29. Iida, Y., Okuyama, K. and Sakurai, K. 1994, International Journal Heat and Mass Transfer, 37(17), 2771.
30. Okuyama, K., Mori, S., Sawa, K. and Iida, Y. 2006, International Journal Heat and Mass Transfer, 49, 2771.
31. Avedisian, C. T., Osborne, W. S., McLeod, F. D. and Curly, C. M. Proceedings of Royal Society, London, A 445, 3875.
32. Kuznetsov, V. V. and Kozulin, I. A. 2010, Journal of Engineering Thermophysics, 19(2), 102.
33. Asai, A., Hara, T. and Endo, I. 1987, Japanese Journal of Applied Physics, 26(10), 1794.
34. Asai, A. 1989, Japanese Journal of Applied Physics, 28(5), 909.
35. Asai, A. 1991, ASME Journal of Heat Transfer, 113, 973.
36. Yin, Z., Prosperetti, A. and Kim, J. 2004, International Journal Heat and Mass Transfer, 47, 1053.
37. Varlamov, Yu. D., Meshcheryakov, Yu. P., Predtechenskii, M. P., Lezhnin, S. I. and Ulýankin, S. N. 2007, Journal of applied Mechanics and technical physics, 48(2), 213.
38. Hong, Y., Ashgriz, N. and Andrews, J. 2004, ASME Journal of Heat Transfer, 126, 259.
39. Xu, J. and Zhang, W. 2008, International Journal Heat and Mass Transfer, 51, 389.
40. Henry, R. D. and Fauske, H. K. 1979, ASME Journal of Heat Transfer, 101, 280.
41. Ochiai, M. and Bankoff, S. G. 1976, Paper No. SNI 6/3, Proceedings of Third Special Meeting on Sodium/Fuel Interactions in Fast Reactors, Tokyo, Japan.
42. Iida, Y., Takashima, T., Watanabe, T., Ohura, H., Ogiso, C. and Araki, N. 1982, Proceedings of 19th National Heat Transfer Symposium of Japan, Nagoya, 511.
43. Gunnerson, F. S. and Cronenberg, A. W. 1978, ANS Annual meeting, Sandiego, USA.

44. Gerweck, V. and Yadigaroglu, G. 1992, International Journal Heat and Mass Transfer, 35, 1823.
45. Inada, S. and Yang, W. J. 1993, International Journal Heat and Mass Transfer, 36, 1505.
46. Elias, E. and Chambre, P. L. 2009, Heat Mass Transfer, 45, 659.
47. Hasan, M. N., Monde, M. and Mitsutake, Y. 2011, International Journal Heat and Mass Transfer, 54, 2844.
48. Kagan, Y. 1960, Russian Journal of Physical Chemistry, 34, 42.
49. Carslaw, H. S. and Jaeger, J. C. 1959, Conduction of heat in Solids, 2nd Edition, Oxford University Press, New York.
50. Zhao, Z., Glod, S. and Poulikakos, D. 2000, International Journal Heat and Mass Transfer, 43, 281.
51. Debenedetti, P. G. 1996, Metastable Liquids: Concepts and Principles, Princeton University Press.
52. Godlesky, E. S. and Bell, K. J. 1966, Proceedings of 3rd International Heat Conf. AIChE, N.Y., 4, 51.
53. Gambill, W. R. and Lienhard, J. H. 1989, ASME Journal of Heat Transfer, 111, 815.
54. Kolev, N. I. 2007, Multiphase Flow Dynamics, 3rd Edition, Vol. 2, Springer, Berlin.
55. Gad-el-Hak, M. 1999, Journal of Fluid Engineering, 121, 690.